Real-time Bacterial Detection by Single Cell Based Sensors Using Synchrotron FTIR Spectromicroscopy**

*Mandana Veiseh, Omid Veiseh, Michael C. Martin, Carolyn Bertozzi, and Miqin Zhang**

[*] Prof. M. Zhang

Department of Materials Science & Engineering

University of Washington

302L Roberts Hall

Seattle, WA 98195-2120

Phone:206-616 9356

Fax: 206-543 3100

E-mail: mzhang@u.washington.edu

Dr. M. Veiseh and Mr. O.Veiseh

Department of Materials Science & Engineering

University of Washington

Dr. M. C. Martin

Advanced Light Source Division

Lawrence Berkeley National Laboratory

Prof. C. Bertozzi

Department of Chemistry

University of California at Berkeley

[**] This work is supported by the University of Washington Engineered Biomaterials Research Center (NSF-EEC 9529161) and through the National Lawrence Berkeley Laboratory ALS Doctoral Fellowship. The Advanced Light Source is supported by the Director, Office of Science, Office of Basic Energy Sciences, Materials Sciences Division, of the U.S. Department of Energy under Contract No. DE-AC03-76SF00098 at Lawrence Berkeley National Laboratory. The facilities at Biological Nanostructures Facility of Molecular Foundry & Materials Sciences Division at Lawrence Berkeley National Lab and UWEB Optical Microscopy and Image Analysis shared resources, funded by the National Science Foundation (grants EEC-9872882 and EEC-9529161) are acknowledged. We also thank the support by Dr. Jie Song and the lab assistance of Vincent Eng, Yumiko Kusumay, Joyce Tseng, Lisamarie Ramos, and Alex Fichtenholtz.

Keywords: Biosensors, Cell adhesion, FTIR, BioMEMS, self-assembled monolayers

Abstract

Microarrays of single macrophage cell based sensors were developed and demonstrated for real time bacterium detection by synchrotron FTIR microscopy. The cells were patterned on gold-SiO_2 substrates via a surface engineering technique by which the gold electrodes were immobilized with fibronectin to mediate cell adhesion and the silicon oxide background were passivated with PEG to resist protein adsorption and cell adhesion. Cellular morphology and IR spectra of single, double, and triple cells on gold electrodes exposed to lipopolysaccharide (LPS) of different concentrations were compared to reveal the detection capabilities of these biosensors. The single-cell based sensors were found to generate the most significant IR wave number variation and thus provide the highest detection sensitivity. Changes in morphology and IR spectrum for single cells exposed to LPS were found to be time- and concentration-dependent and correlated with each other very well. FTIR spectra from single cell arrays of gold electrodes with surface area of 25 μm^2, 100 μm^2, and 400 μm^2 were acquired using both synchrotron and conventional FTIR spectromicroscopes to study the sensitivity of detection. The results indicated that the developed single-cell platform can be used with conventional FTIR spectromicroscopy. This technique provides real-time, label-free, and rapid bacterial detection, and may allow for statistic and high throughput analyses, and portability.

1. Introduction

Cell-based sensors are hybrid systems (biological + device) that use cells' remarkable abilities to detect, transduce, and amplify very small changes of external stimuli.[1] They offer new opportunities for many biomedical applications, including biothreat detection, drug evaluation, pollutant identification, and cell type determination.[2] They are generally constructed by interfacing cells to a transducer that converts cellular responses into detectable signals. Recent years have witnessed a substantial increase in application of planar microelectrode arrays for development of cell-based biosensors (CBBs)[3-5] since they can be easily interfaced with electronic, optical or chemical detecting elements.[6] The success of such CBBs relies primarily on an effective cell patterning technique that can create an addressable array of single or multiple cells with high precision and biostability. Major advantages of these sensing arrays over conventional biosensors include: rapid and inexpensive analyses, minimal sample size requirement, low sample contamination, high throughput, sensitivity, and portability. Among cell-based sensors, single cell arrays are particularly inviting; with an array of virtually identical cells as sensing elements integrated with real-time data acquisition technology, it is possible to experimentally study cellular pathways without interference from other cells, thereby eliminating the uncertainty incurred by neighboring cells.[7] The accurate statistical analysis of cell behavior is questionable without single cell based system, since only highly identical targets may generate meaningful statistical data.[8]

In this study, we developed a cell-based sensor system by combining a microarray of single macrophage cells with synchrotron FTIR spectromicroscopy and demonstrated its sensing ability via real time bacterium detection. Conventional technology for detection and identification of bacteria

using reagent-based tools, including immunoassay, genetic markers, or cell culturing, are slow and/or costly due to the reliance on expensive consumables. For example, salmonella detection takes 3–4 days for presumptive results and 5–7 days for confirmation.[9] The developed technique allows rapid bacterium detection in a few hours. Lipopolysaccharide (LPS) was selected as our model analyte since it is a major structural component of gram-negative bacterial cell wall and a potent activator of cells of the macrophage lineage. LPS is a major pathogenic factor causing septic shock syndrome and death in critically ill patients.[10-13] The syndrome is mainly caused by an overproduction of pro-inflammatory cytokines after macrophage cells are activated by lipopolysaccharide.[14-20] Macrophage activation by LPS and its products are both dose dependent and heterogeneous.[21-23]

A silicon oxide substrate was patterned with an array of gold square electrodes and then surface-modified to host a single or a group of macrophage cells on each electrode. FTIR spectra and optical reflectance DIC images were acquired from cell patterned substrates to study the cell morphology and signals before and after exposure to bacterial LPS. The responses of cells in isolated (single cell), and communicating (colony of the cells) states to bacterial LPS were investigated and compared using synchrotron spectromicroscopy. Additionally, a comparison study was performed for cellular analysis on the spectra generated by synchrotron and conventional FTIR sources to illustrate how the light source quality would affect sensitivity and resolution of the cell-based sensors.

2. Results and Discussion

The process of cellular attachment on the detection platforms is critical, since artifacts may be introduced in the infrared spectra if cells form multiple layers. The process of surface modification for

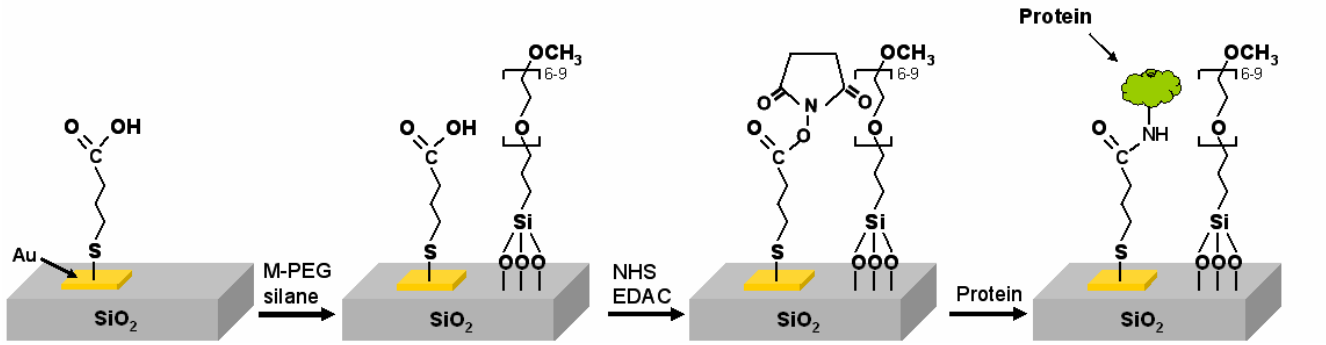

Figure 1. Schematic representation for activation of gold microelectrodes and passivation of silicon background before cell culture, presented in terms of a single gold electrode on a silicon dioxide background.

cellular attachment on gold microelectrodes is illustrated in Figure 1. Each gold microelectrode is activated with an alkane thiol self-assembled monolayer (SAM) and is covalently reacted with cell adhesive proteins through a N-hydroxysuccinimide (NHS) coupling agent. The silicon oxide regions are passivated with methoxy-polyethylene glycol-silane.[24]

In this platform each microelectrode hosts one to three cells depending on the electrode size. As will be shown later, cells will form monolayers.

2.1 Heterogeneous cellular behavior dependent on cell state

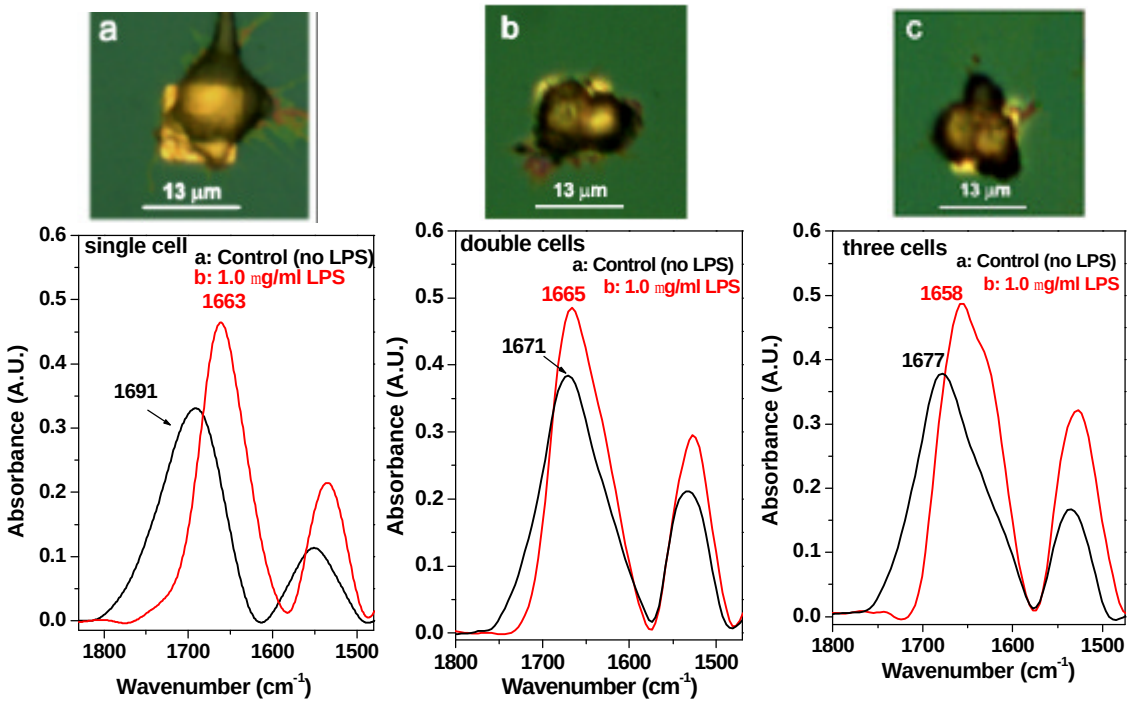

Figure 2. Top panel: Optical DIC images of 100 μm^2 patterns hosting (a) an isolated macrophage cell, and (b) two macrophage cells, and (c) triple cells on a single gold microelectrode after treatment with 1 μg/ml LPS for 21 hrs. Bottom panel: Real-time synchrotron IR spectra of (a) an isolated cell, (b) double cells, and (c) triple cells before and after treatment with LPS.

Cells in an isolated state (for example, one cell in each microelectrode) generally respond differently to external stimuli than when they are in a communicating state (colony of cells on a microelectrode). This is a topic of extensive study in cell biology and an important, but poorly understood issue in the development of cell-based sensors. To reveal this difference, macrophage cells were patterned in singlet, doublet, or triplet on each electrode by culturing substrates with cells of different concentrations. Figure 2 shows the exemplary optical DIC images of these cell patterns (top

panel) and their corresponding IR synchrotron spectra before and after the cells were exposed to LPS at a concentration of 1 μg/ml for 21 hours (bottom panel).

It is noted that the cells in these different states generated different spectra even before exposure to LPS, with, for example, the amide I spectrum peak at 1691 cm^{-1} for cells in singlet state, 1671 cm^{-1} for cells in doublet state, and 1667 cm^{-1} for cells in triplet state. The variation in wave number after cells had been exposed to LPS also differs from state to state, with the cells in the singlet state resulting in the greatest change in wave number and thus providing the highest detection sensitivity.

2.2 LPS induced morphological changes of single macrophage cells

The binding of LPS may induce a variety of responses from macrophages, including the synthesis and secretion of the cytokines, the production of lipid mediators, and cytocidal activities. Macrophage stimulation by LPS is initiated through a complex cascade of bimolecular interactions such as binding of a water-soluble lipopolysaccharide protein (LBP) in serum and forming a protein complex.[14] This complex is then attracted to a cluster of receptors known as the LPS receptor complex expressed on macrophage cell membranes.[13] Upon recognition of LPS by this receptor, a cluster of intercellular transcription factors are transduced to the nucleus leading to an upregulation of various proteins involved in the activation cascade.

Figure 3 shows the optical DIC images of macrophage patterned on the gold microelectrodes after 21 hours of cell culture for (a) control cells with no LPS treatment, and cells treated with LPS at concentrations of (b) 0.1 μg/ml, (c) 1.0 μg/ml, and (d) 10 μg/ml. The results show that macrophage cells cultured with LPS underwent a marked morphological transformation. The control cells exhibited

a small and round shape morphology, while LPS treated cells have an enlarged, dendritic-like shape. This observation is in consistence with the results reported by *Saxena et al.*, when macrophage cells were cultured with LPS on a solid glass slide and exhibited an increased size and the transformation to dendritic-like morphology due to differentiation.[25] Here, this phenomenon was observed for the first

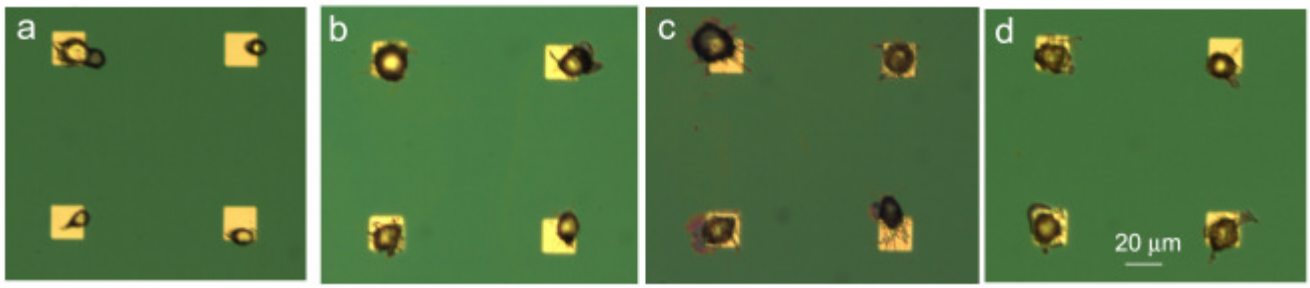

Figure 3. Optical DIC images of macrophage cells cultured on fibronectin-coated surfaces after culture or expose to LPS for 21 hours. (a) Control cells with no LPS treatment, and cells treated with LPS at concentrations of (b) 0.1 µg/ml, (c) 1.0 µg/ml, and (d) 10 µg/ml.

time in a single-cell platform and the morphological transformation was detected *in situ* by FTIR as shown below.

2.3 IR spectral changes of single macrophage cells induced by LPS of various concentrations

Figure 4 (left panel) shows the IR spectra of individual macrophage cells patterned on the microelectrodes, and treated with LPS of different concentrations for 21 hrs. The right panel shows the optical images of the morphology of the cells from which the spectra was acquired. For both panels, (a) corresponds to the cell cultured without PLS (control), and (b) through (d) correspond to the cells cultured with LPS at concentrations of 0.1 µg/ml, 1.0 µg/ml, and 10 µg/ml, respectively.

Images in Figure 4 show that all the LPS-treated cells tend to form dendritic morphology with an increased surface area as the LPS concentration was increased. These morphological changes are accompanied by the changes in IR signature, characterized by the shifts of characteristic bands of amide I and amide II groups of cell proteins in the FITR spectra. The peak associated with the amide I

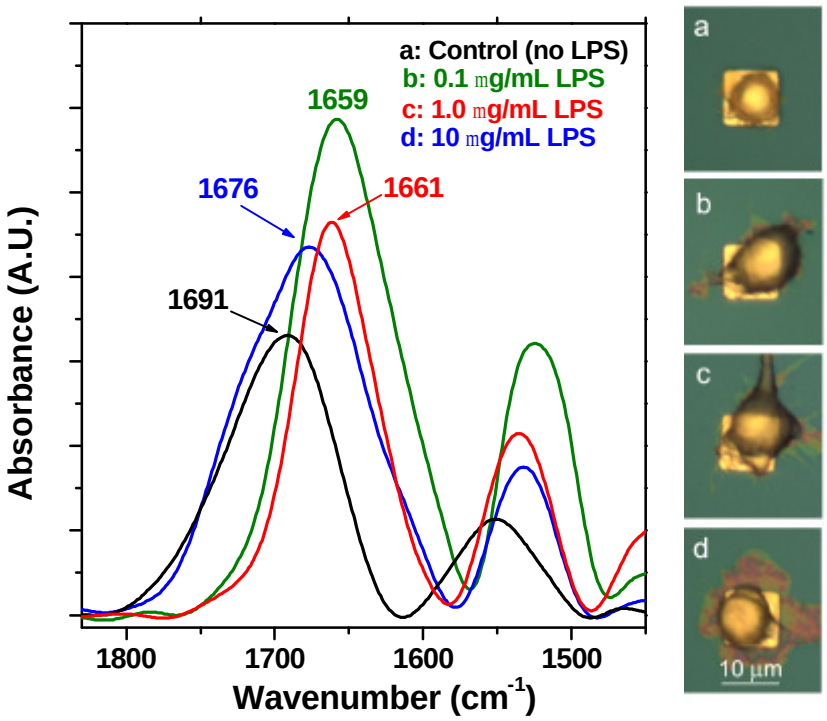

Figure 4. Left panel: real time synchrotron FTIR spectra taken from single macrophage cells patterned on gold electrodes with an area of 100 μm^2. Right panel: optical DIC images of macrophage cells cultured with (a) no LPS, and with LPS at concentrations of (b) 0.1 µg/ml, (c) 1.0 µg/ml, and (d) 10 µg/ml for 21 hrs.

groups (predominantly the C=O stretching vibration of the amide) was shifted from 1691 cm^{-1} for control cells to 1676 cm^{-1} (10 µg/ml LPS), 1661^{-1} (1 µg/ml LPS), and 1659 cm^{-1} (0.1 µg/ml LPS) for

cells treated with LPS. Clearly, the wave number decreases as LPS concentration increases (data on lower concentration were not shown) and reaches a maximum between 0.1 and 1.0 μg/ml. The dramatic differences in the spectra of the amide I between the control and LPS treated cells indicate significant differences in protein structure that might be due to the upregulation of various proteins and peptides involved in the macrophage activation cascade. This result indicates a concentration dependent response of single cells that can be readily detected by FTIR. It is worth noting that a shift of from 2–7 cm^{-1} in wave number has been used to identify diseased tissue from healthy tissues in multi-cell platforms.[6,26] Here a shift in the order of a few tens of wave number (e.g., 30 cm^{-1} observed for the LPS concentration of 1.0 μg/ml), which is considerably greater than the previously reported values, demonstrated a high sensitivity of the single cell based platform reported here. Clearly, such variation in wave number in response to bacterium invasion is sufficient for identification of low volume bacterium invasion and more importantly, the degree of such invasion.

2.4 Time dependent IR spectra changes of single macrophage cells induced by LPS

Figure 5 (left panel) shows IR spectra acquired by synchrotron-based FTIR microspectroscopy from single cells patterned on an array of gold microelectrodes exposed to LPS at a concentration of 1 μg/ml for (b) 3.5 hrs and (c) 21 hrs. A spectrum from control cells (a), i.e., the cells without exposure to LPS, is also shown for comparison. The right panel of Figure 5 shows the optical images of the corresponding cell morphology of the single macrophage cells in the time course. The morphology of the LPS-treated cells was seen to change with LPS exposure time from a spherical to dendritic shape with a significant increase in size after 21 hrs. The corresponding IR spectra of these cells changed as

well over the exposure time, characterized by the noticeable shifts of amide I and amide II bands of the cellular proteins from high to low wave numbers and an increase in signal intensity.

This suggests that the variation in wave number in response to bacterium invasion, as detected using the single-cell platform reported here, is sufficient for identification of a minimal volume of invasive bacterium in a short amount of time (hours vs. days by conventional bacterial detection methods).

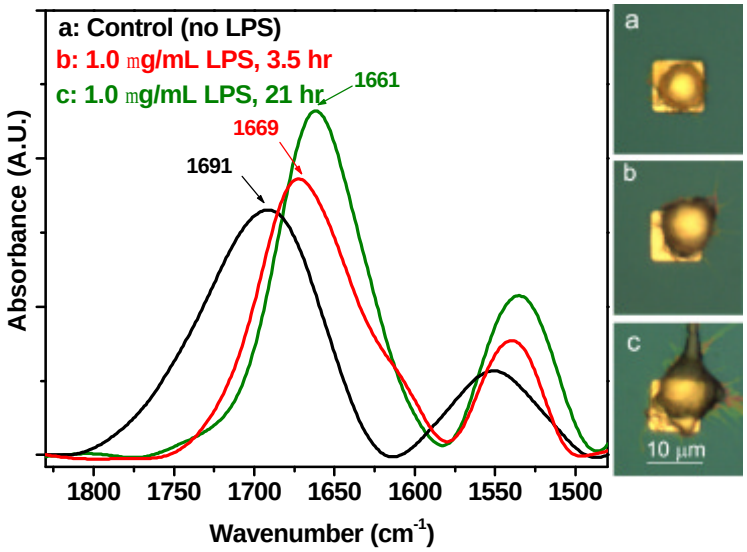

Figure 5. Real time synchrotron IR spectrum of a single cell response to LPS (1.0 µg/ml) for different times.

2.5 Influence of electrode size on detection sensitivity

Signal intensity directly correlates with IR source brightness and the electrode size. In a gold patterned silicon platform maximum signal is obtained when the synchrotron IR focal point is in the

center of gold electrode and the signal attenuation from silicon oxide regions is minimized. The high signal-to-noise ratio and superior brightness of the synchrotron source at a spatial resolution less than 10 microns provide sufficient sensitivity for detection of single cells on the electrodes of 100 μm^2 as shown above. However, a conventional IR thermal source with an effective beam diameter of ~75 μm requires electrodes larger than the beam size to reduce signal loss to surrounding area. To study the sensitivity of detection and the possibility of using conventional FTIR for bacterial detection using the single cell platform, the FTIR spectra from single cell arrays of gold electrodes with surface area of 25 μm^2, 100 μm^2, and 400 μm^2 were acquired using both synchrotron and conventional FTIR spectromicroscopes.

Figures 6A and B show FTIR spectra acquired from single macrophage cells on microelectrodes of different sizes by the synchrotron and conventional FTIR, respectively. The signal intensity increased with the increase in electrode size in both systems. Figure 6A showed that characteristic peaks of cell membranes at wave number of 2800–3600 cm^{-1} and the characteristic peaks of cellular proteins at 1200–1700 cm^{-1} resolved well even for the smallest electrode size with a surface area of 25 μm^2. In spite of a significant signal decrease with the conventional source (Figure 6B), the IR spectral features of a single cell is clearly resolved for the 100 μm^2 and 400 μm^2 microelectrodes. These results indicate that the developed single-cell platform can be used with conventional FTIR spectromicroscopy if the electrode surface areas are larger than 100 μm^2. Although increasing the size of electrodes will increase the signal intensity, it also increases the probability of adhesion of a second cell on an electrode, making single cell patterning more difficult.

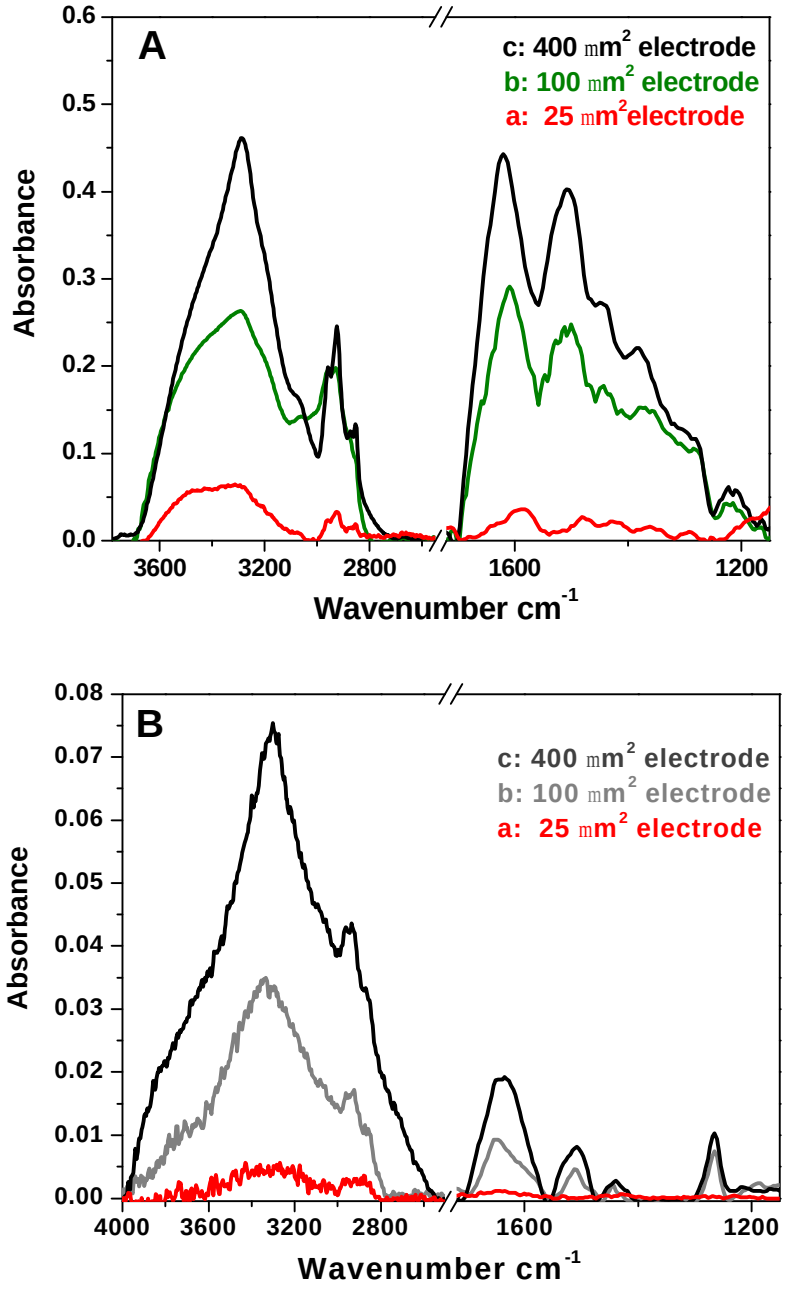

Figure 6. FTIR detection of single macrophage cells adhered on sizes. (A): Synchrotron FTIR spectra and (B) conventional FTIR spectra (aperture size: 90 × 90 μm^2). In both Figure 6A and B, spectrum (a), (b), (c) correspond to 25 μm^2 100 μm^2, and (c) 400 μm^2, respectively.

Conclusions

A live cell array of biosensors was fabricated by immobilizing macrophage cells on gold electrodes on a silicon substrate. The sensor array hosting a single cell on each electrode was found to generate the most significant IR wave number changes in response to bacterial infection compared to multiple-cell sensors and thus provide the highest detection sensitivity. The cells exposed to LPS tended to form dendritic structures with an increased surface area. These morphological changes are accompanied by variations in IR signatures. Changes in morphology and IR spectrum for single cells were found to be time- and concentration-dependent. This technique may provide a time- and cost-effective means to detect and analyze bacterium invasion in a few hours compared to conventional bacteria detection methods in a few days. It may enable the large-scale systematic studies of equally cultured and spread macrophage cells and facilitate the statistical analysis over large numbers of individual functional cells.

3. Experimental

Materials: The following materials and chemicals were used as received: silicon wafers of (100) orientation (Wafernet, CA), Nanostrip 2X (Cyantek, Fremont, CA), 11-mercaptoundecanoic acid 95% (11-MUA), 3-mercaptopropionic acid 99% (3-MPA), N-hydroxysuccinimide 97% (NHS), 1-ethyl-3-(3-dimethylamino-propyl) carbodiimide (EDAC) (Sigma, St. Louis, MO), 2-[methoxy(polyethyleneoxy)propyl] trimethoxysilane (M_w = 460–590 Dalton) (Gelest, Morrisville, PA), fibronectin protein, Trypsin-EDTA, Sigmacote and lipopolysaccharide (*E.-coli* 0111:B4, endotoxin unit: 500,000) (Sigma, Milwaukee, WI). All the solvents including toluene, tri-ethyl amine, and dimethylformamide were purchased from Aldrich (Milwaukee, WI). Absolute ethanol was always

deoxygenated by dry N_2 before use. RAW264.7 cells (murine monocyte/macrophage) were purchased from American Type Culture Collection (Manassas, VA). The following cell cultures reagents were purchased from Gibco (Carlsbad, CA): Trypan Blue, Fetal Bovine Serum, HBSS (Hanks balanced Salt Solution), DMEM (Dulbecco's modified Eagle's medium with 4 mM L-glutamine adjusted to contain 1.5 g/L sodium bicarbonate and 4.5 g/L glucose).

Substrate Preparation: 4" p-type silicon substrates of (100) orientation were cleaned with piranha (hydrogen peroxide/sulfuric acid 2:5 v/v) at 120℃ for 10 min, dipped in HF, and rinsed with DI water thoroughly. A layer of positive photoresist (1.1 μm) was then coated on the surface and patterns were formed on the substrate upon exposure to ultraviolet light through a mask with square patterns of 3 different sizes (25 μm^2, 100 μm^2, and 400 μm^2). A 10 nm titanium (Ti) layer was then deposited onto the photoresist-developed substrates at a deposition rate of 0.3 Å/s. Gold films of 100 nm in thickness were subsequently deposited onto the Ti at a deposition rate of 5 Å/s. A layer of positive photoresist (1.1 μm) was coated on silicon substrates patterned with 3 different sizes of gold squares (25 μm^2, 100 μm^2, and 400 μm^2). The photoresist was dissolved in acetone and the remaining metal films were lifted off. After lift off, the surfaces were exposed to buffered oxide etch (HF/ NH4F 5:1 v/v) for 60 sec and rinsed with DI water to remove native oxide on silicon regions before dry oxidation. Surface oxidation was performed under a dry oxygen flow for 6 hrs at 400°C. The gold-patterned silicon oxide substrates were then cut into 8 mm × 8 mm slides. To minimize surface contaminants and unexpected scratches, the silicon oxide wafers were coated with a 2 μm layer of photoresist on their polished sides before cutting.

Surface Modification: The surface was modified following a previously established procedure with minor modifications.[27,28] The protective photoresist layer on gold-patterned silicon substrates were removed by 10 min sonication in acetone, 2 min sonication in ethanol, and 2 min sonication in DI water. The substrates were then placed in Nanostrip 2X solution (H_2SO_5) at room temperature for 20 min, and dried under nitrogen, which resulted in a hydroxyl layer on the silicon oxide surface.

The gold electrodes of the substrate were first reacted with a 20 mM mixture of alkane thiols of 11-mercaptoundecanoic acid (MUA) and 3-mercaptopropionic acid (MPA) (1:10 v/v) for 16 hrs to create a self-assembled monolayer (SAM). The silicon oxide background was passivated with PEG. The PEG solution was prepared in nitrogen-filled reaction flasks by adding 3 mM methoxy-PEG-silane in deoxygenated toluene containing 1% triethylamine as catalyst. The Nanostrip treated substrate was then placed in a separate nitrogen-filled flask that was rendered hydrophobic with Sigmacote to minimize the side reaction of PEG with the flask. The PEG reaction proceeded under nitrogen at 60°C for 18 hrs. Physically adsorbed moieties were removed from the PEG-treated surface by sonication in toluene and ethanol for 5 min each, followed by rinsing with DI water and drying under nitrogen. The substrate with alkane thiol self-assembled monolayers on gold and M-PEG-silane on silicon oxide background was immersed in an aqueous solution of 150 mM EDAC and 30 mM N-hydroxysuccinimide (NHS) for 30 min to attach the NHS group to the –COOH terminus of SAMs. The substrate with NHS on gold and PEG on silicon oxide was sterilized with 70% ethanol for 15 min, and exposed to fibronectin protein at a concentration of 0.05 mg/ml in a phosphate buffer solution (PBS) of pH = 8.2 at room temperature for 45 min. To remove loosely bound moieties from the surface after each step of the surface modification, the substrate was rinsed with the original solvents and deionized (DI) water, respectively.

Cell Culture: RAW264.7 of passage less than 10 was cultured at 37°C in a 5% CO_2–humidified incubator and grown in DMEM medium supplemented with 10% (v/v) heat-inactivated FBS, 4 mM L-glutamine, 1.5 g/L sodium bicarbonate, 4.5 g/L glucose, 100 units/ml penicillin, and 100 g/ml streptomycin. Cells were subcultured by a cell scrapper. Solutions of lipopolysaccharide were prepared by dissolving lipopolysaccharide (500,000 endotoxin units/mg) from *E.-coli* 0111:B4 in HBSS to a stock concentration of 1 mg/ml. RAW264.7 cells at a concentration of 2.5×10^5 cells/ml in DMEM media were incubated with patterned substrates for 21 hrs and the cell-patterned substrates were then exposed to LPS at a concentrations of 0.1, 1.0, or and 10 µg/ml.

Differential Interference Contrast (DIC) Reflectance Microscopy: Cell culltured surfaces were visulized with a differential interference contrast (DIC) reflectance microscope (Nikon E800 Upright Microscope, NY, NY) equiped with DIC-20× (N.A. 0.46) and DIC-50× (N.A. 0.8) objectives. Images were acquired with a Coolsnap camera (series A99G81021, Roper scientific Inc, AZ, USA) attached to the microscope and a computer.

FTIR Spectromicroscopy: Synchrotron FTIR spectra were acquired from cell-patterned surfaces through a Nicolet Magna 760 FTIR bench and a Nicolet Nic-Plan™ IR microscope with a computer-controlled x–y–z sample stage (via Nicolet Atlµs™ and OMNIC software) and an MCT-A detector at Beamline 1.4.3 of the Advanced Light Source (ALS) in Lawrence Berkeley National Laboratory, Berkeley CA [29,30]. The sample was measured between wave number 650 and 10,000 cm^{-1} set by the KBr or XT-KBr beamsplitter and MCT-A detector ranges. The synchrotron infrared light is focused to

a diffraction-limited spot size with a wavelength-dependent diameter of approximately 3–10 μm across the mid-IR range of interest.[31-33] An on-stage temperature controlled mini incubator was used to maintain a proper environment for cellular analysis. Prior to infrared analysis, the cell culture medium was replaced with fresh sterile medium and the substrate covered with a layer of the medium was transferred to the mini incubator. Synchrotron FTIR spectra of 128 scans at a resolution of 8 cm^{-1} were acquired from individual electrodes patterned with cells. Background spectra were collected from empty surface areas of the same substrate right before data collection. All spectra were baseline-corrected and normalized. An appropriately scaled water vapor spectrum was subtracted from the spectra of the cells. Conventional source FTIR microscopic spectra were obtained from cell-patterned surfaces using a Thermo-Electron Nexus 870 bench and a Thermo-Electron Continuum infrared microscope with an MCT-A detector at Beamline 1.4.4 of the ALS under the same conditions set for the synchrotron measurements, except that an aperture size of 90×90 μm^2 were employed to maximize the signal intensity.

References:

[1] L. Lorenzelli, B. Margesin, S. Martinoia, M. T. Tedesco, M. Valle, *Biosensors & Bioelectronics* **2003**, *18*, 621-626.
[2] R. Bashir, *Advanced Drug Delivery Reviews* **2004**, *56*, 1565-1586.
[3] M. Yang, S. Prasad, X. Zhang, A. Morgan, M. Ozkan, C. S. Ozkan, *Sensors And Materials* **2003**, *15*, 313-333.
[4] X. B. Wang, M. Li, *Assay And Drug Development Technologies* **2003**, *1*, 695-708.
[5] A. van Bergen, T. Papanikolaou, A. Schuker, A. Moller, B. Schlosshauer, *Brain Research Protocols* **2003**, *11*, 123-133.
[6] L. M. Miller, P. Dumas, N. Jamin, J. L. Teillaud, J. Miklossy, L. Forro, *Review Of Scientific Instruments* **2002**, *73*, 1357-1360.
[7] M. B. Elowitz, A. J. Levine, E. D. Siggia, P. S. Swain, *Science* **2002**, *297*, 1183-1186.
[8] H. Hyden, *Trac-Trends in Analytical Chemistry* **1995**, *14*, 148-154.

[9] W. Andrews, *FAO Food Nutr Pap* **1992**, *14*, 1-338.
[10] C. R. H. Raetz, *Annual Review Of Biochemistry* **1990**, *59*, 129-170.
[11] R. J. Ulevitch, P. S. Tobias, *Annual Review Of Immunology* **1995**, *13*, 437-457.
[12] J. Cohen, *Nature* **2002**, *420*, 885-891.
[13] M. Fujihara, M. Muroi, K. Tanamoto, T. Suzuki, H. Azuma, H. Ikeda, *Pharmacology & Therapeutics* **2003**, *100*, 171-194.
[14] R. R. Schumann, S. R. Leong, G. W. Flaggs, P. W. Gray, S. D. Wright, J. C. Mathison, P. S. Tobias, R. J. Ulevitch, *Science* **1990**, *249*, 1429-1431.
[15] H. W. Zhang, J. W. Peterson, D. W. Niesel, G. R. Klimpel, *Journal Of Immunology* **1997**, *159*, 4868-4878.
[16] S. Akashi, R. Shimazu, H. Ogata, Y. Nagai, K. Takeda, M. Kimoto, K. Miyake, *Journal Of Immunology* **2000**, *164*, 3471-3475.
[17] E. Rovida, A. Paccagnini, M. Del Rosso, J. Peschon, P. Dello Sbarba, *Journal Of Immunology* **2001**, *166*, 1583-1589.
[18] C. Soler, R. Valdes, J. Garcia-Manteiga, J. Xaus, M. Comalada, F. J. Casado, M. Modolell, B. Nicholson, C. MacLeod, A. Felipe, A. Celada, M. Pastor-Anglada, *Journal Of Biological Chemistry* **2001**, *276*, 30043-30049.
[19] J. E. Kirkley, B. J. Thompson, J. S. Coon, *Scandinavian Journal Of Immunology* **2003**, *58*, 51-58.
[20] M. Triantafilou, K. Triantafilou, *Journal Of Endotoxin Research* **2003**, *9*, 331-335.
[21] T. A. Hamilton, M. M. Jansen, S. D. Somers, D. O. Adams, *Journal Of Cellular Physiology* **1986**, *128*, 9-17.
[22] N. P. Wiklund, H. H. Iversen, A. M. Leone, S. Cellek, L. Brundin, L. E. Gustafsson, S. Moncada, *Acta Physiologica Scandinavica* **1999**, *167*, 161-166.
[23] M. A. E. Frevel, T. Bakheet, A. M. Silva, J. G. Hissong, K. S. A. Khabar, B. R. G. Williams, *Molecular And Cellular Biology* **2003**, *23*, 425-436.
[24] M. Veiseh, B. T. Wickes, D. G. Castner, M. Q. Zhang, *Biomaterials* **2004**, *25*, 3315-3324.
[25] R. K. Saxena, V. Vallyathan, D. M. Lewis, *Journal Of Biosciences* **2003**, *28*, 129-134.
[26] B. R. Wood, M. A. Quinn, B. Tait, M. Ashdown, T. Hislop, M. Romeo, D. McNaughton, *Biospectroscopy* **1998**, *4*, 75-91.
[27] M. Veiseh, M. H. Zareie, M. Q. Zhang, *Langmuir* **2002**, *18*, 6671-6678.
[28] S. Lan, M. Veiseh, M. Zhang, *Biosens Bioelectron* **2005**, *20*, 1697-1708.
[29] M. C. Martin, R. W. Mckinney, in *Proceed. Mater. Res. Soc., Vol. 524*, **1998**, pp. 11-15.
[30] M. C. Martin, W. R. McKinney, in *Proceedings of the Low Energy Electrodynamics in Solids, '99 Conference, Pécs, Hungary, Special Issue of Ferroelectrics, Vol. 249*, **2001**, pp. 1-10.
[31] G. L. Carr, *Review of Scientific Instruments* **2001**, *72*, 1613-1619.
[32] P. Dumas, N. Jamin, J. L. Teillaud, L. M. Miller, B. Beccard, *Faraday Discussions* **2004**, *126*, 289-302.
[33] E. Levinson, P. Lerch, M. C. Martin, *Infrared Physics and Technology* **2005**, *in press*.

Keywords: Biosensors, Cell adhesion, FTIR, BioMEMS, self-assembled monolayers

Table of content:

Microarrays of single macrophage cell based sensors were developed for real time bacterium detection by synchrotron FTIR sepctromicroscopy. Time- and concentration-dependent morphological and IR spectral changes for single cells exposed to bacterial lipopolysaccharide are demonstrated. This technique provides real-time, label-free, and rapid bacteria detection, and may allow for statistic and high throughput analyses, and portability.